PLATELETS AND THROMBOPOIESIS

# A new form of macrothrombocytopenia induced by a germ-line mutation in the *PRKACG* gene

Vladimir T. Manchev,[1,2,3] Morgane Hilpert,[1,2,3] Eliane Berrou,[4] Ziane Elaib,[4] Achille Aouba,[5] Siham Boukour,[1,3,4] Sylvie Souquere,[3,6] Gerard Pierron,[3,6] Philippe Rameau,[3,7] Robert Andrews,[8] François Lanza,[9] Regis Bobe,[4] William Vainchenker,[1,3] Jean-Philippe Rosa,[4] Marijke Bryckaert,[4] Najet Debili,[1,3] Remi Favier,[1,10] and Hana Raslova[1,3]

[1]Institut National de la Santé et de la Recherche Médicale, Unité Mixte de Recherche 1009, Université Paris-Sud 11, Equipe Labellisée Ligue Contre le Cancer, Villejuif, France; [2]University Paris Diderot, Paris, France; [3]Gustave Roussy, Villejuif, France; [4]Institut National de la Santé et de la Recherche Médicale, Unité Mixte de Recherche_S 770, Université Paris-Sud 11, Le Kremlin Bicêtre, France; [5]Assistance Publique-Hôpitaux de Paris, Médecine Interne-Immunologie Clinique, Antoine Beclere Hospital, Clamart, France; [6]Centre National de la Recherche Scientifique, Unité Mixte de Recherche 8122, Université Paris-Sud 11, Villejuif, France; [7]Plate Forme Imagerie et Cytomètrie de Flux, Integrated Research Cancer Institute in Villejuif, Villejuif, France; [8]Australian Centre for Blood Diseases, Monash University, Melbourne, Australia; [9]Institut National de la Santé et de la Recherche Médicale, UMR S949, Université de Strasbourg, Etablissement Français du Sang Alsace, Strasbourg Cedex, France; and [10]Assistance Publique-Hôpitaux de Paris, Armand Trousseau Children Hospital, French Reference Center for Platelet Disorders, Haematological Laboratory, Paris, France

## Key Points

- We identify a new type of autosomal recessive macrothrombocytopenia associated with a mutation in PRKACG, coding the PKA catalytic subunit.
- The homozygous PRKACG mutation leads to a deep defect in proplatelet formation that was restored by the overexpression of wild-type PRKACG.

**Macrothrombocytopenias are the most important subgroup of inherited thrombocytopenias. This subgroup is particularly heterogeneous because the affected genes are involved in various functions such as cell signaling, cytoskeleton organization, and gene expression. Herein we describe the clinical and hematological features of a consanguineous family with a severe autosomal recessive macrothrombocytopenia associated with a thrombocytopathy inducing a bleeding tendency in the homozygous mutated patients. Platelet activation and cytoskeleton reorganization were impaired in these homozygous patients. Exome sequencing identified a c.222C>G mutation (missense p.74Ile>Met) in *PRKACG,* a gene encoding the γ-catalytic subunit of the cyclic adenosine monophosphate-dependent protein kinase, the mutated allele cosegregating with the macrothrombocytopenia. We demonstrate that the p.74Ile>Met PRKACG mutation is associated with a marked defect in proplatelet formation and a low level in filamin A in megakaryocytes (MKs). The defect in proplatelet formation was rescued in vitro by lentiviral vector-mediated overexpression of wild-type PRKACG in patient MKs. We thus conclude that PRKACG is a new central actor in platelet biogenesis and a new gene involved in inherited thrombocytopenia with giant platelets associated with a thrombocytopathy. (*Blood*. 2014;124(16):2554-2563)**

## Introduction

Inherited thrombocytopenias (ITs) are a heterogeneous group of blood disorders characterized by a reduced platelet count in blood. Some of these diseases are exclusively restricted to megakaryocytes (MKs) and platelets, whereas others also affect other tissues. Functional platelet defects are also often associated, and their severity may lead to a high risk of bleeding. Based on the mean platelet volume, ITs have been classified into 3 subgroups with large, normal, or small platelets.

The most important subgroup of inherited platelet disorders is characterized by low platelet counts and the presence of large and giant platelets, designated as macrothrombocytopenia. This subgroup includes 2 types of thrombocytopenia. The first type is characterized by syndromic features associated with mutations in genes encoding myosin IIA in myosin heavy chain 9 (MYH9)-related disease, filamin-A (FLNa) in FLNa-related thrombocytopenia, friend leukemia integration 1 (FLI1) in Paris-Trousseau syndrome, and ATP-binding cassette sub-familly G member 5 (ABCG5) macrothrombocytopenia associated with sitosterolemia. In contrast, the second type lacks syndromic features and is related to mutations in genes encoding transcription factors such as GATA1 and GFI1B and for cytoskeletal proteins or surface receptors such as tubulin β1, αIIbβ3, and platelet glycoprotein Ib (GPIb)/platelet glycoprotein IX (GPIX).[1,2] Recently, next-generation sequencing methodology led to the identification of the *NBEAL2* gene altered in Gray platelet syndrome[3] and of the *ACTN1* gene affected in congenital macrothrombocytopenia (CMTP).[4]

Here, using exome sequencing, we identified for the first time a c.222C>G mutation in the *PRKACG* gene in a family with a novel form of IT. *PRKACG* encodes the γ isoform of the catalytic subunit

Submitted January 27, 2014; accepted July 9, 2014. Prepublished online as *Blood* First Edition paper, July 24, 2014; DOI 10.1182/blood-2014-01-551820.

V.T.M. and M.H. contributed equally to this work.

R.F. and H.R. contributed equally to this work.

The online version of this article contains a data supplement.

There is an Inside *Blood* Commentary on this article in this issue.

The publication costs of this article were defrayed in part by page charge payment. Therefore, and solely to indicate this fact, this article is hereby marked "advertisement" in accordance with 18 USC section 1734.

(Cγ) of cyclic adenosine monophosphate (cAMP)-dependent protein kinase A (PKA), and the mutation is predicted to lead to a missense p.74Ile>Met substitution. This mutation is responsible for the autosomal recessive IT characterized by defects in proplatelet formation and platelet activation in the homozygous patients, identifying a new mechanism responsible for thrombocytopenia and thrombocytopathy.

## Material and methods

### Patients

Blood samples from patients and healthy subjects were collected after informed written consent was obtained in accordance with the Declaration of Helsinki. The study was approved by the Ethic Committee of the Institut National de la Santé et de Recherche Médicale Recherche Biomédicale (INSERM RBM) 01-14.

### Samples

Venous blood from the patient was collected in 10% (volume to volume) ACD-A buffer (75 mM trisodium citrate, 44 mM citric acid, and 136 mM glucose, pH 4). The platelet-rich plasma was prepared by centrifugation at 80*g* for 10 minutes. Platelets were pelleted by centrifugation at 2100*g* for 10 minutes. Platelets were washed in the presence of apyrase (100 mU/mL) and prostaglandin E1 (1 μM) to minimize platelet activation. The number of platelets from the patient and the control was adjusted to similar levels ($2.5 \times 10^8$ platelets/mL) in Tyrode's buffer (137 mM NaCl, 2 mM KCl, 0.3 mM $NaH_2PO_4$, 1 mM $MgCl_2$, 5.5 mM glucose, 5 mM *N*-2-hydroxyethylpiperazine-*N*′-2-ethanesulfonic acid, 12 mM $NaHCO_3$, and 2 mM $CaCl_2$, pH7.3). For western blot analysis of platelets, remaining red blood cells ($GPA^+$) were depleted using immunomagnetic beads (AutoMACS; Miltenyi Biotec SAS).

Peripheral blood $CD34^+$ cells were separated by double-positive selection using a magnetic cell-sorting system (AutoMACS; Miltenyi Biotec SAS).

### Free intracellular calcium concentration measurement

Washed platelets ($2.5 \times 10^7$ platelets/mL) were loaded with Oregon green 488 BAPTA1-AM (1 μM; Molecular Probes, Eugene, OR) for 45 minutes at 20°C. Platelets were then diluted in Tyrode's buffer to $2.5 \times 10^6$ platelets/mL, and the cytosolic $Ca^{2+}$ concentration was analyzed using an Accuri C6 (Becton Dickinson) flow cytometer. First, $Ca^{2+}$ mobilization in response to thrombin was observed in absence of extracellular $Ca^{2+}$ (100 μM EGTA). After 3 minutes, $Ca^{2+}$ influx was induced by adding $Ca^{2+}$ (300 μM) in extracellular medium.

### Platelet spreading and F-actin/G-actin quantification

Glass coverslips were precoated with human von Willebrand factor (VWF; 10 μg/mL) in the presence of botrocetin (5 μg/mL) and with fibrinogen (100 μg/mL; HYPHEN BioMed SAS) overnight at 4°C. Then washed platelets ($10^7$ platelets/mL; 150 μL) were allowed to adhere at room temperature. After 30 minutes, adherent platelets were fixed with 4% paraformaldehyde in 0.1 M piperazine-N,N′bis(2-ethanesulfonic acid), 2 M glycerol, 1 mM EGTA, and 1 mM $MgCl_2$, pH 6.9, for 15 minutes and then permeabilized in the same buffer containing 0.2% Triton X-100 for 5 minutes. Platelets were stained with both Alexa Fluor488-labeled phalloidin and Alexa Fluor594-labeled DNAse I (Molecular Probes) and then visualized under an epifluorescence microscope (Eclipse 600; Nikon France). Cell surfaces and F- and G-actin contents were determined using ImageJ version 1.42k (rsb.info.nih.gov/ij).

### Targeted exome sequencing (v5-70 Mb)

Library preparation, capture, sequencing, and variant detection were performed by IntegraGen S.A. (Evry, France). Genomic DNA was extracted with the DNA purification kit (Quiagen), captured using Agilent in-solution enrichment methodology with their biotinylated oligonucleotides probes library (Human All Exon v5-70 Mb; Agilent), followed by paired-end 75-base massively parallel sequencing on Illumina HiSEQ 2000. For detailed explanations of the process, see Gnirke et al.[5] Sequence capture, enrichment, and elution were performed according to the manufacturer's instructions and protocols (SureSelect; Agilent). Briefly, 3 μg of each genomic DNA was fragmented by sonication and purified to yield fragments of 150 to 200 bp. Paired-end adaptor oligonucleotides from Illumina were ligated on repaired, A-tailed DNA fragments and then purified and enriched by 4 to 6 polymerase chain reaction (PCR) cycles. Five hundred nanograms of these purified Libraries was hybridized to the SureSelect oligo probe capture library for 24 hours. After hybridization, washing, and elution, the eluted fraction was PCR-amplified with 10 to 12 cycles, purified, and quantified by quantitative PCR to obtain sufficient DNA template for downstream applications. Each eluted-enriched DNA sample was then sequenced on an Illumina HiSEQ 2000 as paired-end 75-base reads. Image analysis and base calling were performed using Illumina Real Time Analysis Pipeline version 1.12 with default parameters.

The bioinformatics analysis of sequencing data was based on the Illumina pipeline (CASAVA1.8.2). CASAVA performs alignment of the reads to a reference genome (hg19) with the alignment algorithm ELANDv2, and then calls the SNPs based on the allele calls and read depth and detects variants. Only the positions included in the oligonucleotide probe coordinates ±20 bp were conserved. Genetic variation annotation was performed using the IntegraGen in-house pipeline, which consists of gene annotation (RefSeq), detection of known polymorphisms (dbSNP 132; 1000Genome), and mutation characterization (exonic, intronic, silent, or nonsense).

For each position, the exomic frequencies (homo and heterozygous) were determined from the IntegraGen exome database and the exome results provided by HapMap.

The *PRKACG* mutation was validated by Sanger sequencing using forward (5′-ACCGCCATGGGCAACGC-3′) and reverse (5′-GAAAACC CACAGGGGCACAA-3′) primers.

### In vitro MK differentiation

Patient or control $CD34^+$ cells were grown in serum-free medium as previously reported.[6] The medium was supplemented with 10 ng/mL thrombopoietin (TPO) (Kirin Brewery) and 25 ng/mL stem cell factor (SCF; Biovitrum AB).

### Flow cytometry analysis

MKs were stained with directly coupled monoclonal antibodies anti–CD41-phycoerythrin and anti–CD42a-allophycocyanin (BD Biosciences) for 30 minutes at 4°C. Platelet surface staining of CD41a, CD42a, and CD62P was performed with the PLT Gp/Receptors kit (Biocytex) at room temperature before and after activation by the thrombin receptor agonist peptide (25 μM). For western blot analysis, MKs were sorted according to CD41 and CD42 expression using an Influx flow cytometer equipped with 5 lasers (BD Biosciences).

### Ploidy analysis

At day 10 of culture, Hoechst 33342 (10 μg/mL; Sigma-Aldrich) was added in the medium of cultured MKs for 2 hours at 37°C. Cells were then stained with directly coupled monoclonal antibodies: anti–CD41-phycoerythrin and anti-CD42a-allophycocyanin (BD Biosciences) for 30 minutes at 4°C.[7] Ploidy was measured in the $CD41^+CD42^+$ cell population by means of an Influx flow cytometer (BD Biosciences) and calculated as previously described.[7]

### Quantification of proplatelets bearing MKs

To evaluate the percentage of MKs forming proplatelets (PPTs) in liquid medium, $CD41^+$ cells were sorted at day 6 of culture and plated in 96-well plates at a concentration of 2000 cells per well in serum-free medium in the presence of TPO (10 ng/mL). MKs displaying PPTs were quantified between

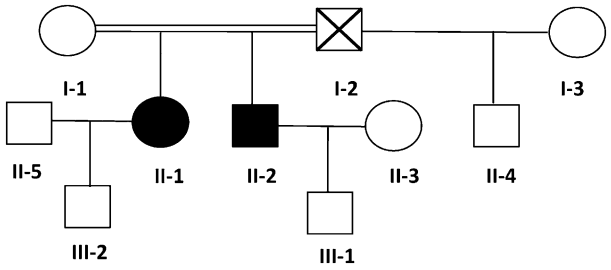


**Figure 1. Family tree**. Circles, females; squares, males; black filled symbols, affected individuals; white symbols, nonaffected individuals; symbol with a diagonal line, deceased individual; double horizontal line, consanguinity.

day 11 and 13 of culture by enumerating 200 cells per well using an inverted microscope (Carl Zeiss) at a magnification of ×200. MKs displaying PPTs were defined as cells exhibiting ≥1 cytoplasmic process with constriction areas (3 wells were examined for each individual and condition).

### Fluorescence microscopy

Fibrinogen (Sigma-Aldrich) was incubated at the concentration of 20 μg/mL on coverslips overnight at 4°C. Primary MKs grown in serum-free medium were plated on coated coverslips for 2 hours at 37°C (5% $CO_2$ in air). Cells were then fixed in 2% paraformaldehyde for 10 minutes, permeabilized with 0.2% Triton X-100 for 5 minutes, and incubated with monoclonal anti-β tubulin (Sigma-Aldrich) and rabbit anti-VWF antibody (Dako) for 1 hour, followed by incubation with Alexa 555-conjugated goat anti-mouse immunoglobulin G (IgG) and Alexa 633-conjugated goat anti-rabbit IgG (Molecular Probes) for 30 minutes. Finally, slides were mounted using Vectashield with 4,6 diamidino-2-phenylindole (Molecular Probes). The PPT-forming MKs (cells expressing VWF) were examined under a Leica DMI 4000, SPE laser scanning microscope (Leica Microsystems) with a 63×/1.4 numeric aperture oil objective. The diameters of platelet-like structures occurring along PPTs were measured with LAS AF version 2.4.1 software, and images were processed using Adobe Photoshop 6.0 software.

### Intraplatelet measurement of cAMP by enzyme-linked immunosorbent assay

Control and patient platelets ($10^7$) were washed as described in the sample section and centrifuged at 2100*g* for 10 minutes at 4°C. Pellets were then resuspended in 200 μL of lysis buffer for 10 minutes at room temperature; 100 μL of the solution was used for the assay performed in duplicate. Intracellular cAMP was measured with the Amersham cAMP Biotrak Enzyme-immunoassay system (GE Healthcare) using the nonacetylation enzyme immunoassay procedure following the manufacturer's recommendation. Optical density was read at 450 nm on a microplate reader (model 680; Bio-Rad), and results were calculated following the manufacturer's recommendation.

### Virus construction and cell transduction

The cDNA of PRKACG was cloned under the promoter EF1α into the bicistronic lentivirus also encoding for the PGK-GFP cassette. The c.222C>G mutation was introduced by directed mutagenesis. Viral particles production and cell transduction were performed, as previously described.[8] Control $CD34^+$ cells ($10^6$/mL) were prestimulated for 24 hours with TPO, interleukin-3, SCF, and Fms-like tyrosin kinase 3-ligand and transduced with concentrated lentiviral (wild-type or mutated PRKACG) particles for 12 hours at a multiplicity of infection of 10, followed by a second transduction. Cells were then cultured in the presence of TPO and SCF alone. $CD41^+GFP^+$ cells were sorted by flow cytometry (FACS Vantage; BD Biosciences) 6 days after transduction. The $CD41^+GFP^+$ cells were further assessed for the ability to form PPTs or for the diameter of PPT-like structures by immunofluorescence assay.

### Western blot assays

MKs were sorted by CD41 and CD42 expression at day 12 of culture, pelleted, and sonicated in 2× Laemli buffer (100 mM Tris-HCl, pH 6.8, 0.05% bromphenol blue, 4% sodium dodecyl sulfate [SDS], and 20% glycerol) supplemented with 100 mM dithiothreitol. Washed unstimulated platelets were lysed in SDS denaturing buffer (50 mM Tris, 100 mM NaCl, 50 mM NaF, 5 mM EDTA, 40 mM β-glycerophosphate, 100 μM phenylarsine oxide, 1% SDS, 5 μg/mL leupeptin, and 10 μg/mL aprotinin, pH 7.4). The proteins were subjected to SDS-polyacrylamide gel electrophoresis and transferred to nitrocellulose. The membranes were incubated with various primary antibodies: affinity-purified rabbit anti–GPIbβ-phospho-$Ser^{166}$ and total rabbit anti-GPIbβ antibodies both previously described,[9] mouse anti–β-actin and anti-HSC70 antibodies (Sigma-Aldrich), mouse anti-PRKACG antibody (Abcam), and rabbit anti-Filamin A antibody (Cell Signaling), followed by horseradish peroxidase-linked secondary antibodies. Protein blots were analyzed using Image Quant LAS 4000 (GE Healthcare), and protein expressions were quantified using ImageQuant TL 8.1 software.

### Electron microscopy

Blood (200 μL) was centrifuged at 2100*g* for 10 minutes in Eppendorf microtubes. Plasma was removed, and the pellet was fixed with 1.5% glutaraldehyde (Fluka Chemie) in 0.1 M phosphate-buffered saline, pH 7.2, for 1 hour at room temperature. The platelet disk was cut into small slices and washed 3 times in 1× phosphate-buffered saline. For morphological examination, fixed platelets were postfixed in 1% osmic acid, dehydrated in ethanol, and embedded in Epon by standard methods.[10] Sections were observed with a Technai 12 transmission electron microscope (FEI).

### Statistical analyses

Data are presented as means ± standard deviation (SD) or ± standard error of the mean (SEM) as indicated. Statistical significance was determined by a 2-tailed Mann-Whitney test or unpaired Student *t* test with Welch's correction. $P < .05$ was considered statistically significant.

## Results

### Family description

A severe thrombocytopenia ($5 \times 10^9$/L) was initially identified after a bleeding episode in 1 21-year-old woman of West Indian origin

**Table 1. Clinical characteristics of *PRKACG*-related thrombocytopenia patients**

| Family member | Age at diagnosis (years) | Current age (years) | Platelet count (×$10^9$/L) | MPV (fL) | Hemoglobin (g/dL) | Leukocytes (×$10^9$/L) | Bleeding score | TPO level (ng/L) |
|---|---|---|---|---|---|---|---|---|
| I-1 | | 44 | 210 | 10.3 | 11 | 4.5 | NB | 35 |
| II-1 | 4 | 23 | 5 | ND | 9 | 5 | 3 | 23 |
| II-2 | 2 | 26 | 8 | ND | 12.3 | 5.6 | 2 | 25 |
| II-3 | | 21 | 229 | 10.8 | 12.9 | 7.1 | NB | 20 |
| III-1 | | 3 | 276 | 10.4 | 10.4 | 8 | NB | 30 |
| III-2 | | 90 d | 277 | 11 | 17 | 14 | NB | ND |

Normal TPO level, <30 ng/L. MPV, mean platelet volume; NB, no bleeding; ND, not done.

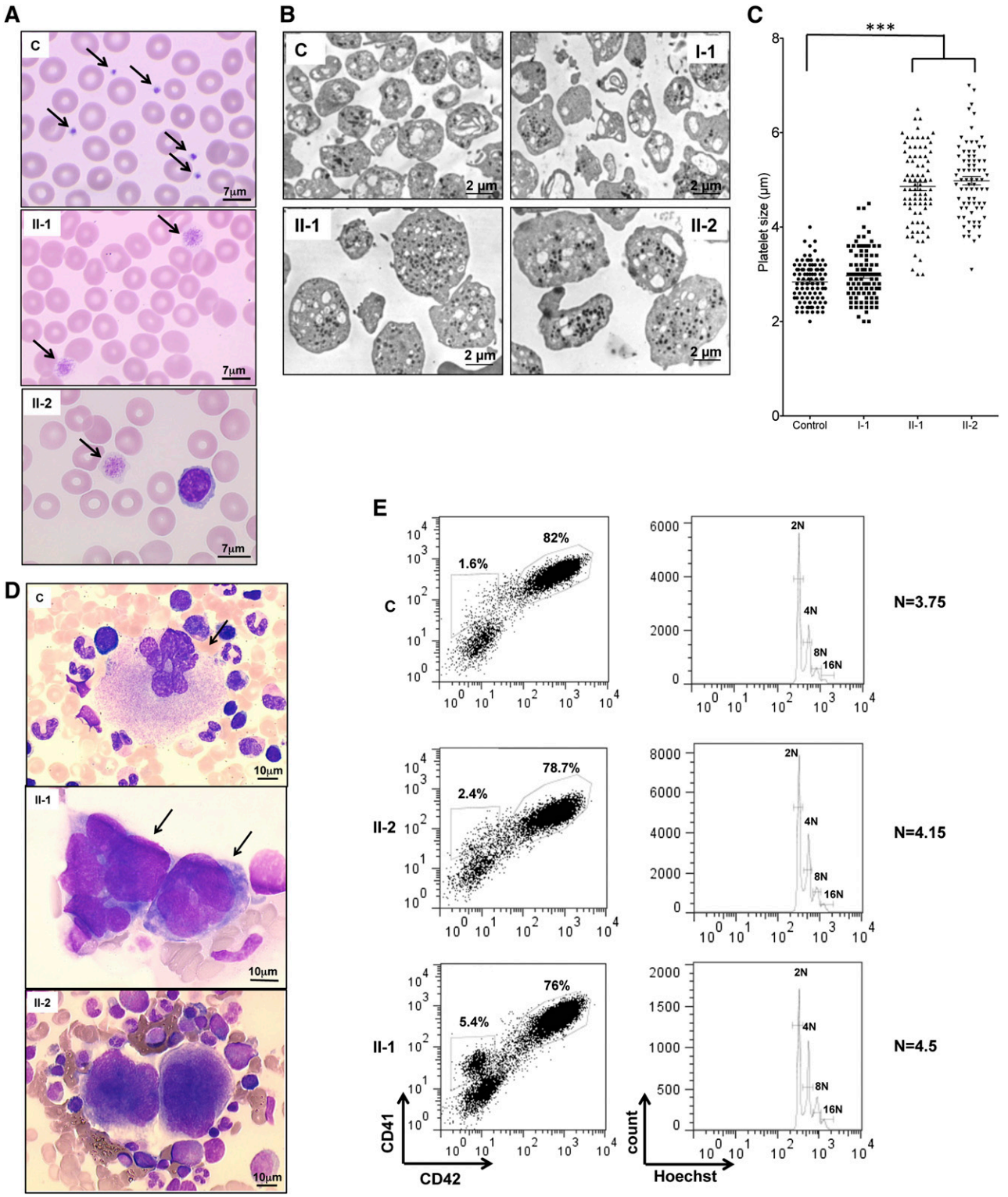


**Figure 2. Platelet and MK analysis.** (A) Cytological investigation of blood platelets. The black arrows point to platelets in the blood smears. Note the much larger platelet size for patients (II-1 and II-2) compared with control (C). (B) Ultrastructural aspect of blood platelets. Large platelets were detected in blood of II-1 and II-2 patients, and platelets of normal size were detected in 1 control and in a I-1 family member with the heterozygous *PRKACG* mutation. (C) The size of 100 platelets for control, I-1, II-1, and II-2 individuals was measured. The results represent mean ± SEM. ***$P < .0001$, unpaired Student *t* test (2-tailed). (D) Cytological investigations of the bone marrow of II-1 and II-2 patients and control. (E) MK differentiation was induced from control or patient peripheral blood $CD34^+$ cells and analyzed at day 10 of culture. Gates represent mature ($CD41^+CD42^+$) or immature ($CD41^+CD42^-$) MKs (left). The ploidy level (N) was analyzed in the gate of $CD41^+CD42^+$ MKs and was based on the percentage of cells in 8N, 16N, and 32N gates.

(proband II-1) at the age of 4 years. She presented with no syndromic features but many bleeding episodes during infancy, including epistaxis, spontaneous hematomas, menorrhagias inducing anemia, and, notably, 3 consecutive bleeding ruptures of ovarian cysts involving life prognosis and requiring platelet and blood cell transfusion. The World Health Organization bleeding score is 4 in this patient.

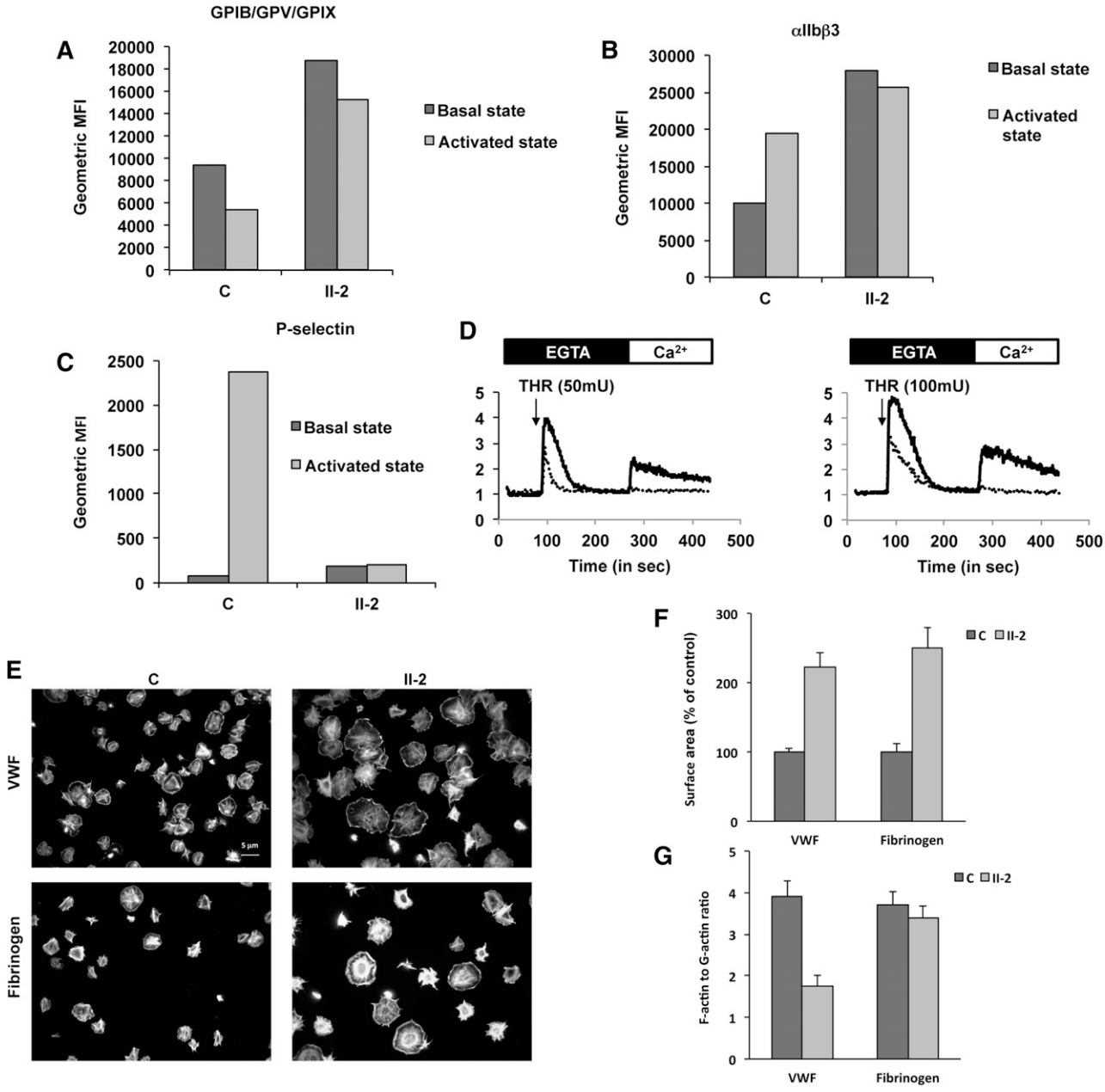


**Figure 3. Platelet functions.** (A-C) Fluorescence-activated cell sorter flow analysis of the (A) GPIb-IX-V complex (anti-CD42a), (B) αIIbβ3 complex (anti-CD41a), and (C) P-selectin (anti-CD62P) on control (C) and patient (II-2) platelets before (basal state) and after activation by thrombin receptor agonist peptide (activated state). Histograms present geometric mean fluorescence intensity (geometric MFI). (D) Typical traces representative of normalized (to basal level) fluorescence intensity of Oregon green 488 BAPTA1-AM (representative of the cytosolic $Ca^{2+}$ concentration) recorded using Accury flow cytometer. Platelets from the control (black line) and from the patient (dotted line) were treated, in the absence of calcium (EGTA, 100 μM), with thrombin (THR, 50 or 100 mU/mL) and $Ca^{2+}$ ($CaCl_2$, 300 μM). (E-G) Platelet spreading. (E) Platelets were adhered on fibrinogen or von Willebrand factor substrates and stained with both Alexa Fluor488-labeled phalloidin and Alexa Fluor594-labeled DNAse I. (F) Platelet surface area and (G) ratio of F-actin to G-actin were measured by ImageJ version 1.42k.

Genealogical studies (Figure 1) showed that her brother (II-2) also exhibited severe thrombocytopenia ($8 \times 10^9$ platelets/L; Table 1) and life-long moderate bleeding, epistaxis, and cutaneous hematomas (World Health Organization bleeding score of 3). Her mother (I-1) had a normal platelet count. Data from her father (I-2) were not available because he died prior to this study. However, his son (II-4) from his second wife (I-3) did not display any platelet defects.

### Platelet and MK morphology

May-Grünwald-Giemsa staining of peripheral blood smears of patients II-1 and II-2 (Figure 2A) showed 90% giant and macrocytic platelets. This was confirmed by electron microscopy. The diameter of platelets was 4.86 and 4.98 μm for II-1 and II-2, respectively, compared with 2.84 and 2.97 μm for control and I-1 platelets, respectively (Figure 2B-C). The morphology of the patient's bone marrow cells revealed the presence of MK clusters, which is absent in normal bone marrow (Figure 2D). An in vitro study of patient MKs derived from peripheral blood $CD34^+$ cells in the presence of TPO and SCF revealed no differences in percentage of mature $CD41^+CD42^+$ cells and in the ploidy level between patients II-1 and II-2 and a healthy donor (Figure 2E). Similar results were obtained for family members I-1 and III-1 (data not shown). Altogether, these results suggest no defect in MK differentiation and ploidization.

### Patient platelets exhibit defective activation

Because the patients exhibit a bleeding score of 3 to 4, suggesting a profound defect in platelet function, we first analyzed the effects of stimulating platelets. Quantification of integrin αIIbβ3 and GPIb/IX/V by flow cytometry showed that their levels in the unstimulated patient platelets was 2.7- and 2-fold higher than in control platelets, respectively (Figure 3A-B), consistent with their large size. After stimulation with protease-activated receptor 4-activating peptide (25 μM), GPIb/XI/V underwent poor activation-dependent internalization (18% of the level of resting platelets) in patient platelets compared with control platelets (44.2% of the level of resting platelets; Figure 3A). Moreover, although surface expression of integrin αIIbβ3 in control platelets, as expected, was upregulated (193% compared with unstimulated control platelets), no change in αIIbβ3 surface expression was observed for patient platelets after stimulation (Figure 3B). Finally, no surface expression of P-selectin, a marker of α granule mobilization, on activation was observed in patient platelets (Figure 3C). Altogether, these results are consistent with patient platelets being unable to undergo activation.

Consistent with altered activation, $Ca^{2+}$ mobilization from internal stores and $Ca^{2+}$ influx elicited by added extracellular $Ca^{2+}$ were much lower in patient platelets upon stimulation with thrombin (50 and 100 mU) than in control platelets (Figure 3D).

Finally, we analyzed platelet spreading with VWF (10 μg/mL) and fibrinogen (100 μg/mL) and quantified actin polymerization by measuring the F-actin/G-actin ratio. Immunofluorescence imaging showed that patient platelets were heterogeneous in morphology (Figure 3E). The majority of the platelets were giant, whereas some of them were of normal size and aspect. Moreover, patient platelets exhibited ruffles, which were absent from the control platelets. Quantification showed that the extent of patient platelet spreading was 2.2- and 2.5-fold that of control platelets with VWF and fibrinogen, respectively (Figure 3F). This larger size is the likely consequence of the larger diameter of the patient platelets vs control platelets. In contrast, a low F-actin/G-actin ratio of patient platelets was observed with VWF (44% of the control), whereas the ratios were comparable with fibrinogen (Figure 3G) between control and patient platelets.

Altogether, these results show an unexpected defect in activation and in cytoskeleton reorganization of patient platelets.

### Homozygous *PRKACG* and *GNE* mutations are present in affected family members

The absence of genetic defects in GPIbα, GPIbβ, and GPIX (expressed as a GPIb-IX complex) excluded Bernard-Soulier syndrome (BSS), and the absence of neutrophil inclusions excluded an MYH9-related disease.[11] Therefore, to identify a genetic factor leading to this new form of macrothrombocytopenia, we performed whole-exome sequencing of family members I-1, II-1, II-2, II-3, and III-1. A total of 57 447 single nucleotide variations (SNVs) and 6781 insertion-deletions (indels) were detected in I-1; 58 351 SNVs and 6968 indels in II-1; 57 341 SNVs and 6832 indels in II-2; 58 129 SNVs and 7077 indels in II-3; and 57 863 SNVs and 7012 indels in III-1. After excluding variants present in public databases at a frequency of >1%, by keeping only nonsynonymous mutations and by imposing an autosomal recessive mode of transmission for the mutation (I-1 and III-1, heterozygous for the mutation; II-1 and II-2, homozygous for the mutation; II-3, homozygous wild type due to the consanguinity between I-1 and I-2 pedigrees and the fact that pedigrees II-4 and III-1 have a normal platelet count), only 2 variations remained. Both are localized on chromosome 9. The first one, c.1675G>A, is in the gene *GNE* and corresponds to the substitution of the amino acid glycine for arginine at position 559 (p.559G>R-NM_005476). The second mutation, c.222C>G, was found in the *PRKACG* gene and substitutes isoleucine for methionine at position 74 (p.74I>M-NM_002732; Figure 4). None of the mutations were found in the SNPdb database, indicating they are not polymorphisms. Furthermore, when analyzed using PolyPhen2, both the GNE p.559G>R mutation and the PRKACG p.74I>M mutation were predicted to be damaging with high probability. Additionally, both residues are well conserved through evolution, further suggesting a strong impact for the mutations. *GNE* encodes a bifunctional enzyme that initiates and regulates the biosynthesis of *N*-acetylneuraminic acid, and *PRKACG* encodes the γ isoform of the catalytic subunit (Cγ) of cAMP-dependent PKA. Among PKA substrates, FLNa and GPIbβ are present in MKs and platelets and are potential candidates involved in thrombocytopenia. Indeed, genetic alterations of FLNa and GPIbβ were found to be associated with macrothrombocytopenia,[1,12] whereas *GNE* mutations result in myopathy or sialuria[13,14] without thrombocytopenia. Because neither myopathy nor sialuria was detected in the patients, we further focused on PRKACG.

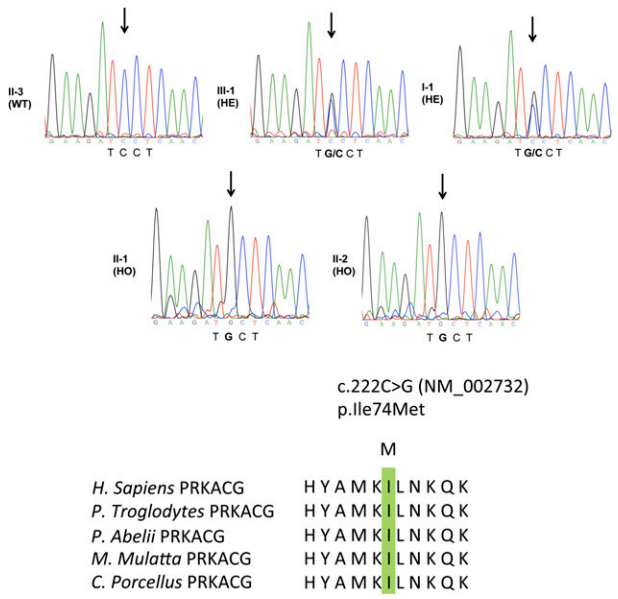


**Figure 4. Germ-line *PRKACG* mutation.** Electrophoregram of *PRKACG* gene (NM_00273), as sequenced by the Sanger method, revealed no mutation in individual II-3 designed as wild type (WT). Individuals III-1 and I-1 were found to be heterozygous (HE) for the c.222C>G mutation, without clinical features of macrothrombocytopenia. Patients II-1 and II-2 were found to be homozygous for the c.222C>G mutation and exhibited macrothrombocytopenia. The c.222C>G mutation caused substitution of the evolutionarily conserved Ile amino acid. Homologous sequences were aligned using the CLUSTALW Web site.

### *PRKACG* homozygous mutation leads to a functional defect of PKA

To ascertain the role or *PRKACG* mutation in the induction of this new autosomal recessive macrothrombocytopenia with giant platelets, we first investigated mutant protein function. First, we found that the *PRKACG* mutation did not lead to the degradation of PRKACG in MKs or platelets (supplemental Figure 1). Then, the phosphorylation status of GPIbβ at $Ser^{166}$ in patient MKs was investigated using $CD34^+$ progenitors cultured in the presence of TPO and SCF and $CD41^+CD42^+$ MKs for 12 days. Quantification showed no difference in P-$Ser^{166}$-GPIbβ levels between homozygous patients and controls in mature MKs (Figure 5A). Moreover, phosphorylation of GPIbβ at $Ser^{166}$ in homozygous patient platelets was comparable to control platelets (Figure 5B). These results suggest that

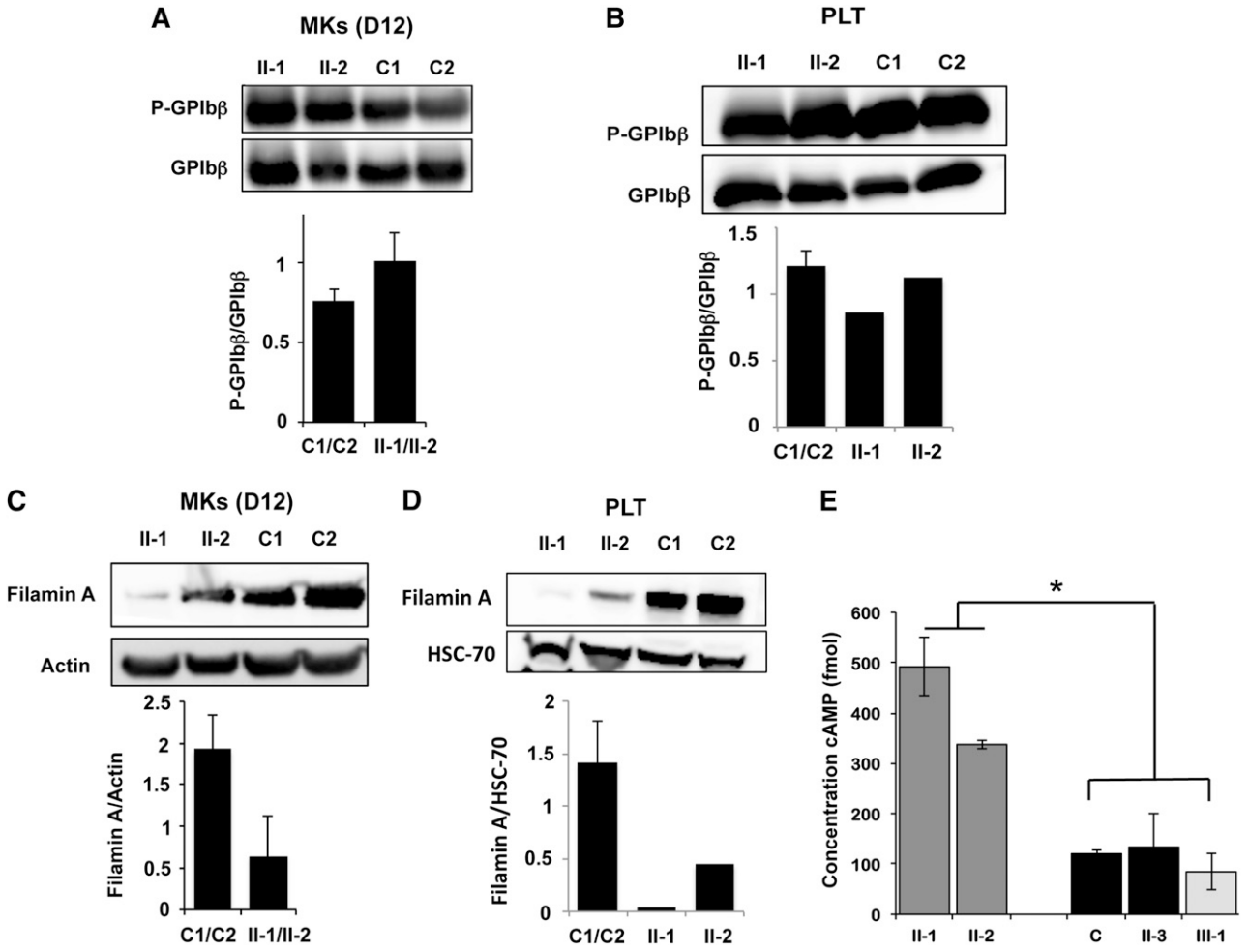


**Figure 5. Analysis of PKA activity in patient platelets and megakaryocytes.** (A-B) Western blot analysis and quantification of GPIbβ phosphorylated at $Ser^{166}$ in MKs derived in vitro from (A) blood $CD34^+$ progenitors and (B) in platelets of patients homozygous (II-1 and II-2) for the PRKACG p.74I>M mutation. Two external controls (C1 and C2) were analyzed. Total GPIbβ was used as a control of protein loading. MKs were investigated at (A) day 12 of culture. (C-D) Western blot analysis and quantification of filamin A in (C) MKs and (D) platelets of patients carrying the homozygous (II-1 and II-2) mutation. Two external controls (C1 and C2) were used. Actin or HSC70 was used as a control of protein loading. (E) Analysis of cAMP level in platelets isolated from one external (C1) and one internal control (II-3) and from 2 patients homozygous (II-1 and II-2) and 1 heterozygous for the PRKACG p.74I>M mutation (III-1). Error bars represent mean ± SD of triplicate. Experiments were performed 2 times with similar results. *$P <$ .05, 2-tailed Mann-Whitney test.

PRKACG is not responsible for GPIbβ phosphorylation in mature MKs and platelets. Finally, because the phosphorylation of FLNa by PKA at $Ser^{2152}$ has been suggested to protect FLNa from proteolysis,[15,16] we examined the level of total FLNa in MKs and platelets. FLNa was almost completely absent from mature MKs (harvested at day 12 of culture) (Figure 5C) and from platelets (Figure 5D) of homozygous patients compared with controls, strongly suggesting that PRKACG is required for FLNa phosphorylation.

The phosphorylation of many substrate proteins by PKA depends on cAMP. PKA regulates the concentration of cAMP as part of a feedback mechanism.[17] First, PKA can induce degradation of cAMP through activation of phosphodiesterases, which catalyze the conversion of cAMP into AMP. Second, PKA can inhibit cAMP synthesis by inhibiting adenylyl cyclase, which catalyzes the conversion of ATP into cAMP. Hence, we hypothesized that the p.74I>M PRKACG mutation alters PKA activity, thereby leading to a high intracellular level of cAMP. Therefore, we measured the cAMP levels in platelets from 1 external and 1 internal control (II-3), from 2 patients homozygous for the PRKACG p.74I>M mutation (II-1 and II-2), and from 1 individual heterozygous for the mutation (III-1). A three- to fivefold higher level of cAMP was detected for patients homozygous for the mutation compared with controls or with a heterozygous individual (Figure 5E).

In conclusion, low amounts of FLNa in both megakaryocytes and platelets and higher cAMP levels in platelets of homozygous patients are strikingly consistent with the PRKACG p.74I>M mutation inactivating PKA.

### PPT formation is defective in patient MKs and is rescued by wild-type PRKACG overexpression

Finally, because the thrombocytopenia was not associated with defective MK differentiation or ploidization (Figure 2D-E), we investigated the ability of patient MKs to produce PPTs. A 2.5-fold lower percentage of PPT-bearing MKs ($CD41^+CD42^+$) was evidenced in patients homozygous for the mutation (II-1 and II-2) compared with controls or with patients heterozygous for the mutation (I-1 and III-1; Figure 6A). To confirm the implication of the homozygous PRKACG p.74I>M mutation in the PPT formation defect, we cloned the wild-type *PRKACG* cDNA into a lentiviral vector and transduced $CD34^+$ cells isolated from peripheral blood of homozygous patients II-1 and II-2. Overexpression of wild-type

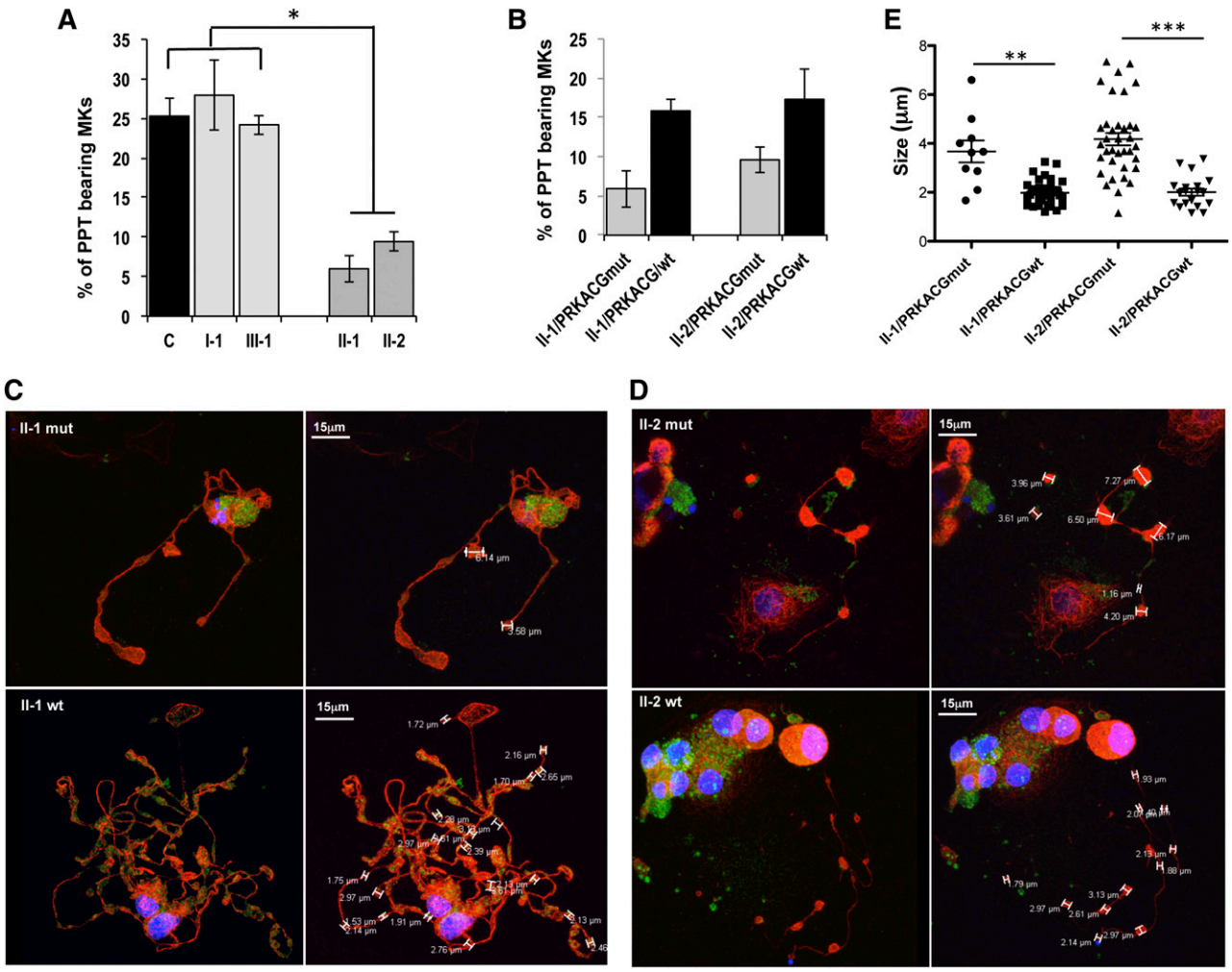


**Figure 6. Mutant PRKACG leads to defective PPT formation, which is rescued by wild-type PRKACG overexpression.** (A-E) In vitro MK differentiation was induced from control or patient peripheral blood $CD34^+$ progenitors in the presence of TPO and SCF. (B-E) $CD34^+$ cells of patients II-1 and II-2 were transduced with a lentiviral vector harboring wild-type (wt) or mutant PRKACG cDNA (used as a control of experiment) at days 1 and 2 of culture. (A-B) The percentage of PPT-forming MKs was estimated by counting MKs exhibiting ≥1 cytoplasmic processes with areas of constriction at day 13 of culture. A total of 200 cells per well were counted. The histograms show 1 of 2 independent experiments with similar results. Each experiment was performed in triplicate. Data represent mean ± SD of triplicate. $^*P < .05$, 2-tailed Mann-Whitney test. (C-D) Immunoconfocal analysis of platelet-like structures formed by PPTs generated from patients (C) II-1 and (D) II-2. MKs overexpressing wt or mutant PRKACG PPT-forming MKs were allowed to adhere on fibrinogen for 2 hours at day 13 of culture and stained with anti-tubulin (red) and rabbit anti-VWF (green) antibodies. Confocal imaging was performed on a Leica TCS SP8 inverted laser scanning confocal microscope (Leica Microsystems, Heidelberg, Germany), equipped with a 405-nm UV laser diode and visible optically pumped semiconductor lasers (488 and 552 nm). All images were acquired using an oil immersion 63× objective (1.4 numeric aperture). (E) At least 5 MKs for each condition were analyzed, and the size of platelet-like structures was measured by LAS AF version 2.4.1 software. Data are presented ± SEM. $^{**}P < .005$ and $^{***}P < .0001$, unpaired Student *t* test with Welch's correction.

PRKACG significantly increased PPT formation by MKs of both patients II-1 and II-2 (Figure 6B). The mutant PRKACG cDNA was used in parallel as a negative control. No rescue in PPT formation was observed in the MKs of patients II-1 and II-2, which already express endogenous mutant PRKACG. Moreover, after overexpression of wild-type PRKACG in patient MKs, the average diameter of platelet-like structures occurring along the PPTs decreased from 3.67 to 1.68 µm for patient II-1 and from 4.17 to 2.01 µm for patient II-2 (Figure 6C-E). This result strongly suggests that the defect in PKA is responsible for the thrombocytopenia.

## Discussion

Here we report a new autosomal recessive macrothrombocytopenia characterized by a severe thrombocytopenia (5-8 × $10^9$ PLT/L) and a severe thrombopathy with a bleeding score of 3 to 4. Exome sequencing revealed homozygous mutations in the coding exons of 2 genes: *GNE* and *PRKACG*. The corresponding GNE p.559G>R and PRKACG p.74I>M missense mutations were predicted by PolyPhen2 to be damaging with high probability, at positions with well-conserved residues, and not corresponding to polymorphisms. GNE is predominantly expressed in the liver and placenta. *GNE* mutations can result in 2 human disorders: myopathy with mutations in epimerase and/or kinase domains or sialuria linked to the mutations in the epimerase domain.[13,14] The GNE p.559G>R mutation located within the kinase domain was reported in 1 patient with myopathy in association with the V572L mutation on the other allele, which is the most frequent mutation associated with this disorder.[18] No thrombocytopenia was ever reported in patients with myopathy and, conversely, the patients described here have no signs of myopathy, suggesting that the GNE p.559G>R mutation induces no major functional defect. Thus, the PKA mutation appears more relevant to explain this thrombocytopenia. PKA is composed of

2 catalytic subunits and 2 regulatory subunits. After cAMP binding to the regulatory subunits, the catalytic subunits dissociate and phosphorylate their substrates. The 3 catalytic subunit isoforms, Cα, Cβ, and Cγ, are present in platelets, with a twofold lower level for Cγ compared with Cα and Cβ.[19] Among the major platelet PKA substrates, 2 groups were identified. The first group includes signaling regulators (Rap1B, Rap1GAP2, $G\alpha_{13}$, $IP_3$-R, TRPC6, and GPIbβ), whereas the second includes actin-binding proteins (VASP, LASP, HSP27, FLNa, and caldesmon).[20] We focused our attention on 2 PKA substrates: FLNa and GPIbβ. Indeed, genetic alterations of these substrates led to different forms of macrothrombocytopenia. Mutations in the *FLNA* gene localized on chromosome X result in a moderate thrombocytopenia with a mix of normal and giant platelets and with a defect in PPT formation.[12] We demonstrated here that the level of total FLNa in PKA patient platelets was drastically low. This could be a consequence of a decrease in FLNa phosphorylation at $Ser^{2152}$ in platelets and MKs due to the defect in PKA activity. This nonprotection of FLNa from proteolysis could then lead to thrombocytopenia. Indeed, we previously showed in patients with mutated FLNa that low levels of remaining FLNa in platelets (30%) are correlated with abnormal fragmentation of the cytoplasm, leading to a defect in PPT formation.[12]

In platelets, GPIb-IX-V, the major receptor for VWF, is constitutively associated with FLNa. This FLNa-GPIbα interaction is required for adhesion of platelets onto VWF at high shear conditions, probably via dimerization and/or links with the actin networks,[21-24] and seems to regulate the mechanical stability of the platelet plasma membrane. In the patient homozygous for the PRKACG p.74Ile>Met mutation, a decrease in F-actin polymerization was observed after platelet spreading on the VWF matrix. This defect is the likely consequence of the absence of stabilization of actin networks by the remaining FLNa.

GPIb-IX-V is another PKA substrate, essential for platelet activation and formation. Indeed, mono-allelic mutations in *GP1BB* are at the origin of autosomal dominant macrothrombocytopenia in BSS characterized by the presence of large platelets.[1] In platelets, PKA mediates GPIbβ phosphorylation at $Ser^{166}$, which leads to the negative regulation of VWF binding to GPIb-IX-V.[9] Moreover, phosphorylation of GPIbβ inhibits actin polymerization during platelet activation through reorganization of the GPIb-IX–associated membrane skeleton.[25] In platelets from the patient homozygous for the PRKACG p.74Ile>Met mutation, GPIbβ phosphorylation was normal; thus, the defect in actin polymerization is not the result of altered GPIbβ but more likely of the degradation of FLNa.

Is the markedly altered activation of platelets, as evidenced by impaired $Ca^{2+}$ mobilization, no αIIbβ3 and P-selectin externalization, and poor GPIb internalization, consistent with PKA inactivation? An attractive hypothesis is that increased intracellular cAMP, observed in patient platelets and a long-time recognized physiological negative regulator of platelet responses,[26-28] alters platelet functions. However, another hypothesis, not exclusive from the first one, is that the defect in FLNa alters actin cytoskeletal reorganization on platelet stimulation, inducing defective externalization or internalization of receptors or even $Ca^{2+}$ translocation. Further experiments are required to test these hypotheses.

GPIb-IX-V central involvement in platelet formation has been demonstrated in 2 ways: antibodies directed against GPIb-IX-V have been shown to strongly inhibit PPT production, and MKs derived from patients with BSS (lacking normal expression of GPIb-IX-V) do not develop PPTs in vitro.[29-31] However, no defect in the phosphorylation of GPIbβ was observed at 12 days of culture, a stage where MKs start to generate PPTs and to release platelets. This suggests that another PKA catalytic subunit rather than PRKACG is involved in GPIbβ phosphorylation.

In conclusion, a new homozygous mutation in the *PRKACG* gene affecting PKA function results in a new form of severe macrothrombocytopenia designated here as *PRKACG*-related disease. This study further demonstrates the potential diagnostic value of exome sequencing in human thrombocytopenia, as well as providing unique evidence for a key role for PKA in normal platelet production and platelet functions.

## Acknowledgments

The authors thank the patients and their families for participation in this study, Genethon (Evry, France) for the sinpRRL-PGK-GFP lentivirus vector, and the Laboratoire Français de Fractionnement et Biotechnologies (LFB, Courtaboeuf, France) for human purified von Willebrand factor.

This work was supported by French grants from the Agence Nationale de la Recherche (Jeunes Chercheurs) (to H.R.) and the Ligue Nationale Contre le Cancer (équipe labellisée 2013) (to H.R.). R.F., N.D., and W.V. are recipients of a research fellowship from Assistance Publique-Hôpitaux de Paris-Institut National de la Santé et de la Recherche Médicale (R.F.), Centre Hospitalier Universitaire Bordeaux (N.D.), and Institut Gustave Roussy-Institut National de la Santé et de la Recherche Médicale (W.V.).

## Authorship

Contribution: V.T.M., M.H., E.B., S.S., G.P., and P.R. performed experiments and analyzed data; Z.E. and S.B. performed experiments; A.A. performed clinical and biological follow-up of patients; R.A., F.L., and W.V. discussed results and wrote the paper; J.-P.R. analyzed data, discussed results, and wrote the paper; R.B., M.B., and N.D. performed experiments, analyzed data, discussed results, and wrote the paper; R.F. performed clinical and biological follow-up of patients, performed experiments, and wrote the paper; and H.R. designed the work, performed and supervised experiments, and wrote the paper.

Conflict-of-interest disclosure: The authors declare no competing financial interests.

Correspondence: Hana Raslova, INSERM, UMR1009, Gustave Roussy, 114 rue Edouard Vaillant, 94805 Villejuif Cedex, France; e-mail: hraslova@igr.fr.

## References

1. Balduini CL, Savoia A, Seri M. Inherited thrombocytopenias frequently diagnosed in adults. *J Thromb Haemost.* 2013;11(6):1006-1019.
2. Stevenson WS, Morel-Kopp MC, Chen Q, et al. GFI1B mutation causes a bleeding disorder with abnormal platelet function. *J Thromb Haemost.* 2013;11(11):2039-2047.
3. Albers CA, Cvejic A, Favier R, et al. Exome sequencing identifies NBEAL2 as the causative gene for gray platelet syndrome. *Nat Genet.* 2011;43(8):735-737.
4. Kunishima S, Okuno Y, Yoshida K, et al. ACTN1 mutations cause congenital macrothrombocytopenia. *Am J Hum Genet.* 2013;92(3):431-438.
5. Gnirke A, Melnikov A, Maguire J, et al. Solution hybrid selection with ultra-long oligonucleotides

for massively parallel targeted sequencing. *Nat Biotechnol.* 2009;27(2):182-189.

6. Debili N, Massé JM, Katz A, Guichard J, Breton-Gorius J, Vainchenker W. Effects of the recombinant hematopoietic growth factors interleukin-3, interleukin-6, stem cell factor, and leukemia inhibitory factor on the megakaryocytic differentiation of CD34+ cells. *Blood.* 1993;82(1): 84-95.
7. Lordier L, Bluteau D, Jalil A, et al. RUNX1-induced silencing of non-muscle myosin heavy chain IIB contributes to megakaryocyte polyploidization. *Nat Commun.* 2012;3:717.
8. Gilles L, Guièze R, Bluteau D, et al. P19INK4D links endomitotic arrest and megakaryocyte maturation and is regulated by AML-1. *Blood.* 2008;111(8):4081-4091.
9. Bodnar RJ, Xi X, Li Z, Berndt MC, Du X. Regulation of glycoprotein Ib-IX-von Willebrand factor interaction by cAMP-dependent protein kinase-mediated phosphorylation at Ser 166 of glycoprotein Ib(beta). *J Biol Chem.* 2002;277(49): 47080-47087.
10. Anderson DR. A method of preparing peripheral leucocytes for electron microscopy. *J Ultrastruct Res.* 1965;13(3):263-268.
11. Savoia A, De Rocco D, Panza E, et al. Heavy chain myosin 9-related disease (MYH9 -RD): neutrophil inclusions of myosin-9 as a pathognomonic sign of the disorder. *Thromb Haemost.* 2010;103(4):826-832.
12. Nurden P, Debili N, Coupry I, et al. Thrombocytopenia resulting from mutations in filamin A can be expressed as an isolated syndrome. *Blood.* 2011;118(22):5928-5937.
13. Argov Z, Mitrani-Rosenbaum S. The hereditary inclusion body myopathy enigma and its future therapy. *Neurotherapeutics.* 2008;5(4):633-637.
14. Bork K, Reutter W, Weidemann W, Horstkorte R. Enhanced sialylation of EPO by overexpression of UDP-GlcNAc 2-epimerase/ManAc kinase containing a sialuria mutation in CHO cells. *FEBS Lett.* 2007;581(22):4195-4198.
15. Jay D, García EJ, Lara JE, Medina MA, de la Luz Ibarra M. Determination of a cAMP-dependent protein kinase phosphorylation site in the C-terminal region of human endothelial actin-binding protein. *Arch Biochem Biophys.* 2000;377(1): 80-84.
16. Chen M, Stracher A. In situ phosphorylation of platelet actin-binding protein by cAMP-dependent protein kinase stabilizes it against proteolysis by calpain. *J Biol Chem.* 1989;264(24):14282-14289.
17. Brown KM, Lee LC, Findlay JE, Day JP, Baillie GS. Cyclic AMP-specific phosphodiesterase, PDE8A1, is activated by protein kinase A-mediated phosphorylation. *FEBS Lett.* 2012; 586(11):1631-1637.
18. Cho A, Hayashi YK, Monma K, et al. Mutation profile of the GNE gene in Japanese patients with distal myopathy with rimmed vacuoles (GNE myopathy). *J Neurol Neurosurg Psychiatry.* 2013.
19. Burkhart JM, Vaudel M, Gambaryan S, et al. The first comprehensive and quantitative analysis of human platelet protein composition allows the comparative analysis of structural and functional pathways. *Blood.* 2012;120(15):e73-e82.
20. Smolenski A. Novel roles of cAMP/cGMP-dependent signaling in platelets. *J Thromb Haemost.* 2012;10(2):167-176.
21. Nakamura F, Pudas R, Heikkinen O, et al. The structure of the GPIb-filamin A complex. *Blood.* 2006;107(5):1925-1932.
22. Cranmer SL, Pikovski I, Mangin P, et al. Identification of a unique filamin A binding region within the cytoplasmic domain of glycoprotein Ibalpha. *Biochem J.* 2005;387(Pt 3):849-858.
23. Williamson D, Pikovski I, Cranmer SL, et al. Interaction between platelet glycoprotein Ibalpha and filamin-1 is essential for glycoprotein Ib/IX receptor anchorage at high shear. *J Biol Chem.* 2002;277(3):2151-2159.
24. Cranmer SL, Ashworth KJ, Yao Y, et al. High shear-dependent loss of membrane integrity and defective platelet adhesion following disruption of the GPIbα-filamin interaction. *Blood.* 2011;117(9): 2718-2727.
25. Fox JE, Berndt MC. Cyclic AMP-dependent phosphorylation of glycoprotein Ib inhibits collagen-induced polymerization of actin in platelets. *J Biol Chem.* 1989;264(16):9520-9526.
26. Salzman EW. Cyclic AMP and platelet function. *N Engl J Med.* 1972;286(7):358-363.
27. Siess W. Molecular mechanisms of platelet activation. *Physiol Rev.* 1989;69(1):58-178.
28. Noé L, Peeters K, Izzi B, Van Geet C, Freson K. Regulators of platelet cAMP levels: clinical and therapeutic implications. *Curr Med Chem.* 2010; 17(26):2897-2905.
29. Takahashi R, Sekine N, Nakatake T. Influence of monoclonal antiplatelet glycoprotein antibodies on in vitro human megakaryocyte colony formation and proplatelet formation. *Blood.* 1999;93(6): 1951-1958.
30. Balduini A, Malara A, Balduini CL, Noris P. Megakaryocytes derived from patients with the classical form of Bernard-Soulier syndrome show no ability to extend proplatelets in vitro. *Platelets.* 2011;22(4):308-311.
31. Machlus KR, Italiano JE Jr. The incredible journey: From megakaryocyte development to platelet formation. *J Cell Biol.* 2013;201(6): 785-796.